Appl. Phys. B 74, 509–515 (2002)
DOI: 10.1007/s003400200797

Applied Physics B
Lasers and Optics

High-order-harmonic generation: towards laser-induced phase-matching control and relativistic effects

P. BALCOU[1,✉]
R. HAROUTUNIAN[1]
S. SEBBAN[1]
G. GRILLON[1]
A. ROUSSE[1]
G. MULLOT[1]
J.-P. CHAMBARET[1]
G. REY[1]
A. ANTONETTI[1]
D. HULIN[1]
L. ROOS[2]
D. DESCAMPS[2]
M.B. GAARDE[2]
A. L'HUILLIER[2]
E. CONSTANT[3]
E. MEVEL[3]
D. VON DER LINDE[4]
A. ORISCH[4]
A. TARASEVITCH[4]
U. TEUBNER[5]
D. KLÖPFEL[5]
W. THEOBALD[5]

[1] Laboratoire d'Optique Appliquée, ENSTA – Ecole Polytechnique, CNRS Unité Mixte de Recherches 7639, 91761 Palaiseau cedex, France
[2] Department of Physics, Lund Institute of Technology, PO Box 118, 22100 Lund, Sweden
[3] CELIA, Université de Bordeaux 1, Cours de la Libération, 33405 Talence, France
[4] Institut für Laser- und Plasmaphysik, Universität-GHS-Essen, 45117 Essen, Germany
[5] Institut für Optik und Quantenelektronik, Friedrich-Schiller-Universität Jena, Max-Wien Platz 1, 07743 Jena, Germany

Received: 5 December 2001
Published online: 24 April 2002 •

ABSTRACT We present a review of some recent results on high-order-harmonic generation, aiming at optimizing the photon flux to allow for future applications in extreme-ultra-violet non-linear optics. We first present new schemes to control phase matching of high harmonics in gases, by using the effect of the spatially varying atomic phase displayed by the high harmonics. An enhancement by a factor of 50 is observed in neon in conditions for which the gradient of the atomic dispersion balances the electronic dispersion. A new scheme to manipulate the laser field was demonstrated, and shown to improve phase matching. We then turn to high-harmonic generation by solid targets, and show that high harmonics generated by an intense 30-fs laser pulse remain collimated even at the threshold of the relativistic regime.

PACS 32.58.Rm; 42.65 Ky; 42.65 Re; 52.40 Nk

1 Introduction

Generation of high-order harmonics is now widely considered as a useful source of extreme ultra-violet (XUV) radiation, with nice properties of spatial collimation and femtosecond temporal resolution. One of the most important advantages of this process is the simplicity of the experimental setup to generate the harmonics: one simply focuses an intense, short-pulse laser onto a target, which can be either a noble-gas medium or a solid target, for instance fused silica. Due to various non-linear processes in the medium, high harmonics are emitted in the laser direction for gases, and in the specular direction for solids. These processes present a high degree of coherence, meaning that most of the laser coherence properties should be retained in the XUV. One may expect therefore to obtain a low-power but high-repetition-rate laser-like source in the extreme ultra-violet spectral region.

One of the main focuses of present-day investigations concerns the optimization of the photon flux. Indeed, the possibility to induce non-linear processes directly in the far-UV range seems very appealing, but it requires fluxes obviously higher than those available today. As a first step, several groups have developed harmonic generation in gases with guiding in a hollow-core fiber [1–4]. A perfect phase-matching regime is then obtained at low ionization probabilities, when the positive atomic dispersion compensates the rising negative free-electron dispersion. We show here that other approaches can also give very interesting results, especially if one makes use of the 'atomic phase' displayed by the harmonics [5].

As concerns high-harmonic generation by solid targets, a limited number of experiments have been performed, even though the photon fluxes are expected to be much higher than with gases [6]. The laser intensities required are indeed also much higher, so that fewer laser facilities are available for such studies. One of the most interesting recent results is certainly the study by Norreys et al. [7] using a picosecond excimer laser. It has shown harmonics of quite high orders, namely around 75, but which display an unexpected very wide angular distribution, possibly due to laser-induced ripples on the surface. We have explored whether or not harmonics generated in the same range of intensities, but in a 30-fs regime, display the same angular behavior [8].

The present paper is organized as follows. We first introduce for non-specialist readers the basics of high-harmonic generation in gases. We then present a new approach of high-

✉ E-mail: balcou@ensta.fr

harmonic generation in a gas cell, for which an impressive enhancement is observed in neon, which is currently interpreted as due to a novel phase-matching regime. We present next a means to improve phase matching and even select one harmonic with respect to the others, simply by manipulating the fundamental field using birefringent optics. We eventually present data of high-harmonic generation from solid targets, showing that, in contrast to other experiments, those harmonics can remain well collimated even close to relativistic intensities.

2 Basics of high-harmonic generation in gases

The existence of high harmonics generated from intense laser pulses focused in noble gases was first demonstrated in 1988 in Saclay and Chicago. Most spectra have a very similar shape, displaying a regular decrease of the harmonic yields for the first few orders, followed by a long spectral range, known as the plateau, where the harmonics show about the same intensities, up to a sudden and final drop, dubbed the cutoff. Heavy noble gases allow one to generate few harmonics, but with quite high conversion efficiencies (often of the order of 10^{-6}); on the other hand, the light noble gases, neon and helium, allow one to generate many harmonics up to very high orders, but with reduced conversion efficiencies (less than 10^{-8}).

Harmonic generation is a process of non-linear optics, in which the electric fields generated by the different atoms add coherently. The final electric field scales therefore as the number density of atoms N, and the harmonic yield as its square. Note however that this argument assumes implicitly that all the atomic dipoles add constructively; whether or not this is indeed the case is known as phase matching, and imperfect phase matching may complicate very seriously the simple N^2 dependence just mentioned.

For symmetry reasons, high harmonics can be generated in linear polarization of the laser, but not in circular polarization. One simple way to understand this is to consider the atom in a frame rotating synchronously with the laser electric field in circular polarization. The laser field is then seen as constant, so that a static response is induced, which, once transformed back to the laboratory frame, yields an atomic response at the laser frequency only. As a result, the harmonics are usually linearly polarized, although they can also be elliptically polarized. Some suggestions were recently proposed to generate purely circularly polarized high harmonics, using media for which the rotation symmetry is broken. No corresponding experimental demonstration has been reported yet.

In media with inversion symmetry, like gas media, only odd harmonic orders are generated. This is simply related to the fact that the atomic response is self-similar every laser half-cycle, but with a change of direction. In contrast, high harmonic generation on solid surfaces displays both even and odd orders, because the surface possesses no inversion symmetry.

As most non-linear processes, the components of the atomic dipoles at high harmonic frequencies increase strongly with the driving laser intensity I. However, this increase is by no means given by a perturbative I^q law, where q is the harmonic order. Phenomenologically, one observes that the increase is steep when the harmonic belongs to the cutoff region of the spectrum, and much slower once it reaches the plateau (often I^3 to I^5 effective power laws are correct fits to the data). The process is ultimately limited by the onset of ionization saturation at high intensities.

Several models have been proposed to explain the very occurrence of high harmonics generated by individual atoms. The most successful one, known as the three-step model, or the semi-classical model, is illustrated by Fig. 1.

In a first step, one outer shell electron of the atom may undergo tunnel ionization through the Coulomb barrier lowered by the laser field. The 'time' taken to go through the barrier should be much shorter than the laser cycle, which means that ionization occurs predominantly in the so-called tunneling regime. In a first approximation, the ionized electron can be considered as born in the continuum with null velocity. In a second step, it is accelerated by the laser field and follows a typical trajectory of a free electron. This trajectory may or may not cross the position of the parent ion, depending on the initial time of ionization. This is illustrated in Fig. 1 in the frame of a freely oscillating electron with no drift velocity. In that frame, it is the atom that oscillates back and forth, and a free electron will follow a straight line, whose slope corresponds to the electron-drift velocity. The zero absolute velocity of the ionized electron at the time of ionization implies that the electron straight line and the atom sine motion should be exactly tangential at the moment of ionization. It is

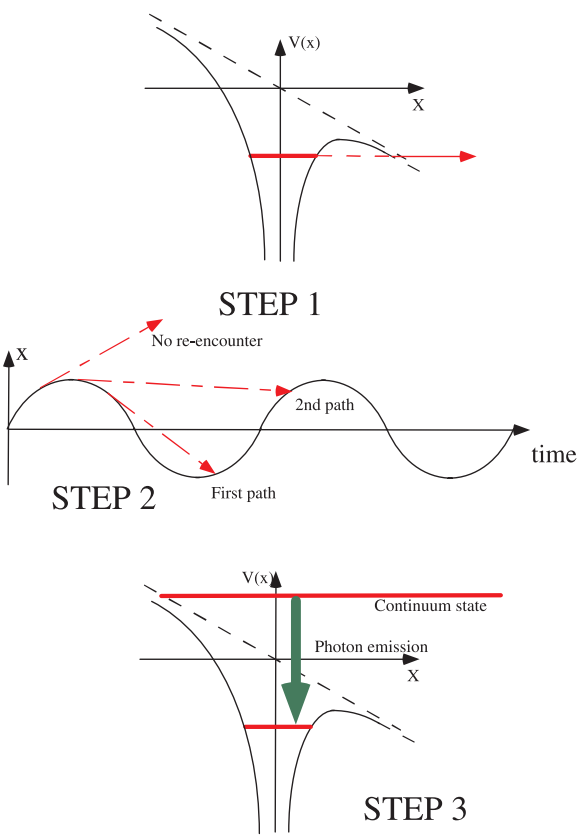

FIGURE 1 Schematic of the three-step model for harmonic generation in gases. Step 1, tunnel ionization; step 2, acceleration in the continuum, along a trajectory viewed in the frame of an oscillating free electron; step 3, radiative recombination

then straightforward to observe in the graph that an electron ionized before the maximum of the laser electric field within the optical cycle will not re-encounter its parent ion, while one ionized at the top of the cycle or after it will collide with the ion. At that moment, radiative recombination has a finite probability to occur, yielding an attosecond flash of light. The quantum repetition of this process every half-cycle results in a high-harmonics spectrum.

From that semi-classical picture, it stems that the maximum photon energy emitted corresponds to the sum of the ionization potential of the atom I_p plus the maximum kinetic energy gained by the electron in the continuum:

$$h\nu = I_p + 3.17U_p\,, \tag{1}$$

where U_p is the well-known ponderomotive potential (average quiver energy). This limit corresponds to the experimentally observed cutoff. For energies lower than this maximum, it is also clear from Fig. 1, step 2, that there always exist two electron trajectories that will result in identical relative velocities at the moment of collision, and hence in identical kinetic and photon energies. Conversely, each harmonic in the plateau can be generated by either of these two trajectories, known as the two main quantum paths.

Finally, it is crucial to note that the harmonic emitted along one path is not in phase with the driving laser field, but presents a phase lag with respect to it, mostly due to the accumulated quantum phase of the electron in the continuum.

This phase lag, known as the atomic or intrinsic phase Φ_{at}, is given to first order by:

$$\Phi_{at} = -\alpha I \tag{2}$$

where I is the laser intensity and α is a numerical coefficient depending on which quantum path is considered. As an example, emission at an intensity of 5×10^{14} W/cm^2 will result in an atomic phase $\Phi_{at} = -127$ rad along the second quantum path. This effect can therefore be very strong; it can be viewed as a giant cross-phase modulation of the laser on the generated harmonics. This will have profound impacts on phase matching.

3 Phase matching in higher-density plasmas using the atomic phase

Optimizing the yield of high-harmonic generation through improvement of phase matching is crucial to get to a regime where XUV non-linear optics is possible. However, one should keep in mind that a global optimization implies optimizing both the microscopic and macroscopic responses.

Microscopically, the polarization at harmonic frequency $q\omega$ is ultimately limited by ionization:

$$P_{q\omega} = d_{q\omega}\,(1 - P_{\text{ionization}}) \tag{3}$$

where $d_{q\omega}$ is the induced dipole moment for an un-ionized atom and $P_{\text{ionization}}$ is the ionization probability of the atom. Increasing the laser intensity leads to the ionization saturating: as the ionization probability goes to one, the polarization drops to zero. This happens at an intensity known as the saturation intensity for ionization, I_{sat}. I_{sat} increases when the pulse duration decreases, so that shorter pulses allow one to increase harmonic orders and yields. If the maximum laser intensity is smaller than I_{sat}, then the atomic polarization remains for the whole pulse, and is maximal at the top of the pulse. On the other hand, laser intensities higher than I_{sat} will lead to a harmonic emission occurring only in the leading edge of the pulse, but with a maximum value much higher than in the previous case. The pulse-intensity value optimizing the single-atom maximum can be expected to be close to saturation, when the ionization probability reaches levels around 50%.

Macroscopically, the optimization of harmonic yields depends on the quality of phase matching. Several terms contribute to the overall dispersion: the weak positive atomic gas dispersion, the strong negative electronic dispersion, the Gouy phase of a focused laser beam, which is equivalent to another negative dispersion, and finally the atomic phase of the harmonic dipole moment. The last can indeed play an important role in phase matching, provided it varies spatially.

In the case of a freely propagating laser beam in a gas jet, all these contributions vary in space in the focal region. This has long had dramatic effects on phase matching: if the laser and one harmonic happen to be phase-matched at one point in the medium, then they will probably not stay phase-matched after some propagation, and the global phase-matching factor is not at all optimized.

This point is instrumental to explain the success of two recently proposed methods to obtain phase matching of high harmonics: hollow-core fibers [1–4] and thin tubes [9].

Using hollow-core capillary fibers makes all the different dispersion factors homogeneous along the fiber: the gas density is uniform provided the fiber is fed with gas from both sides and the laser intensity is uniform (if higher transverse modes have been suppressed, and if attenuation stays negligible). As a result, the free-electron density should be homogeneous, and the atomic phase constant along the axis. In contrast to a common belief, the Gouy phase does exist in a fiber, but it is simply linear, and hence also plays a constant role. Obtaining phase matching at one point implies therefore that it will be kept until the exit of the fiber. The conversion efficiency may then be limited by gas re-absorption [4].

The idea underlying the use of very thin gas media is similar: phase-matched generation should be completed over a very small distance, say 200 μm, before deleterious spatial variations become prohibitive.

In both cases, the physical principle underlying phase matching is to balance the negative electronic dispersion and the Gouy phase by the positive atomic dispersion. However, the atomic dispersion is much weaker than the electronic dispersion, so that the release of very few electrons is sufficient to balance the atomic dispersion. For example, the ionization probability at balance is around 8% in xenon and only 1% in neon. As a result, this scheme for phase matching implies the use of low intensities with respect to the saturation intensity, and the single-atom response is not optimized.

In a very interesting study, Tamaki et al. have proposed to use gas cells [10]. The gas density is constant within a gas cell, which should help a lot; however, the laser propagation is free, so that intensity-dependent and Gouy phases are bound to vary. However, it is in principle possible to combine several

such spatially varying factors, in such a way that the sum of all remains flat over some extended range.

In order to explore this possibility, one may introduce generalized phase-matching conditions, that allow one to consider in a uniform way dispersion terms and spatially dependent phases [11]. We introduce an effective wavevector $\boldsymbol{K}$, which is the gradient of the atomic phase: $\boldsymbol{K} = \nabla\Phi_{\mathrm{at}}$.

The generalized phase-matching condition reads:

$$\boldsymbol{k}_q = q\boldsymbol{k}_1 + \boldsymbol{K}\,, \tag{4}$$

where $\boldsymbol{k}_q$ is the harmonic wavevector, and where the local laser wavevector $\boldsymbol{k}_1$ takes into account the effects of focusing, of atoms and of free electrons: $\boldsymbol{k}_1 = n_1\frac{\omega}{c}\boldsymbol{e}_z + \nabla\Phi_{\mathrm{Gouy}}$, ω being the laser angular frequency, c the speed of light, $\boldsymbol{e}_z$ the unit vector in the propagation direction and n_1 the refractive index at ω including the atomic and electronic contributions.

The quality of phase matching in a given configuration can then be assessed by the magnitude of the remaining wavevector mismatch:

$$\delta k = \left|\boldsymbol{k}_q\right| - \left|q\boldsymbol{k}_1 + \boldsymbol{K}\right| \tag{5}$$

In Fig. 2, we plot one such phase-matching map, calculated with parameters corresponding to the experimental results presented next. The laser-propagation axis is central to the figure, along the abscissa; the radial direction is along the ordinate, on either side of the axis. Gray levels indicate the local value of δk, from white ($\delta k = 0$) to dark gray ($\delta k = 50\ \mathrm{mm}^{-1}$).

In the very specific conditions of ionization probability and of laser intensity chosen in Fig. 2 ($P = 20\%$ and $I = 8\times10^{14}\ \mathrm{W/cm^2}$ for the present focusing conditions), a large area of very good phase matching appears on axis between $z = 2$ mm and $z = 4$ mm after the focus, i.e. in an area where the gradient of the atomic phase acts as a strong positive dispersion. This indicates that, locally, the gradient of the atomic phase compensates for a large electronic dispersion, which should result in very high conversion efficiencies if a gas cell is placed at the corresponding position.

These theoretical predictions were compared with an experiment in which a 1-kHz, 5-mJ, 35-fs Ti–sapphire laser was focused in a gas cell of neon. The harmonics were analyzed by an on-axis Rowland spectrometer, with a very good spectral resolution but a rather low throughput. To avoid any damage to the spectrometer grating submitted to a kHz laser, we used an aluminum foil of 250 nm to protect the spectrometer; as a result, harmonics beyond the aluminum cutoff at 17 nm could not be observed.

Figure 3 presents a spectrum obtained in Ne under optimized conditions. Plateau harmonics, of orders between 19 and 31, can barely be separated: this apparent noise is however clearly a continuum of unresolved harmonics, as the signal at any position scales with pressure and laser intensity like a harmonic. The striking feature is that harmonics from 33 to 45 suddenly rise above the plateau, with a marked bell shape. This behavior is very spectacular, and has long been expected as resulting from phase matching a definite group of harmonics. Note that it is only observed when the cell is located 2 mm after the focus, i.e. if the laser intensity within the cell is decreasing, as predicted by Fig. 2.

To know whether this spectral feature does indicate phase matching, we measured how the signal from harmonic 37 scales with gas pressure and medium length. The results are presented in Fig. 4a and b respectively, on a double-logarithmic plot.

The pressure dependence first increases slowly, then steeply as the pressure reaches values around 20 Torr. The harmonic photon number N_q depends on pressure P through:

$$N_q = KP^2\left|F_q^2\right| \tag{6}$$

where F_q is the phase-matching factor and K is a numerical constant unrelated to pressure. F_q depends a priori on pressure. If it was roughly constant, then the number of harmonic photons should scale as P^2. The straight line in Fig. 4a shows therefore a quadratic increase for comparison. The increase is obviously steeper than a quadratic law between 22 and 40 Torr, which indicates that the phase-matching factor undergoes a large increase. Some improvement of phase matching is therefore achieved, but this result alone does not prove perfect phase matching.

The dependence on length L is presented in Fig. 4b. Length dependences are in principle more simple to inter-

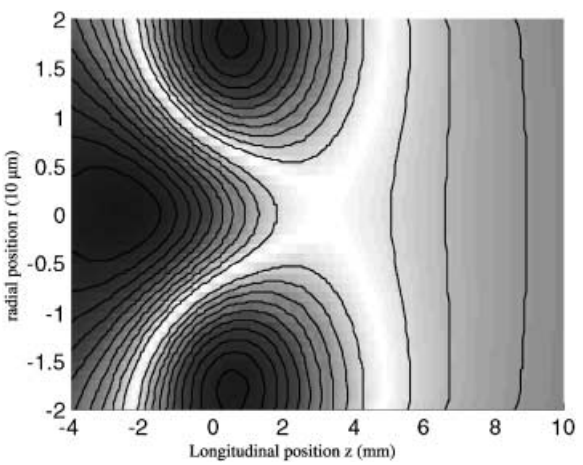

FIGURE 2 Phase-matching map, showing the residual wavevector mismatch in gray levels. White, $\delta k = 0$; dark gray, $\delta k = 50\ \mathrm{mm}^{-1}$. The laser axis is horizontal at the figure center

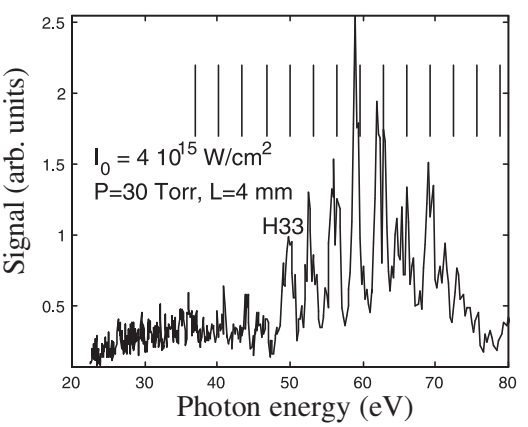

FIGURE 3 Neon spectrum obtained in optimum conditions, with a 4-mm-long gas cell

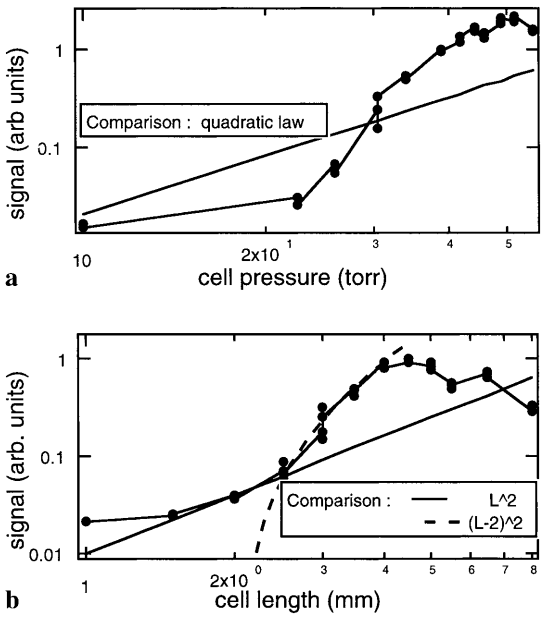

FIGURE 4 Pressure (**a**) and cell-length L (**b**) dependences of 37$^{\text{th}}$-harmonic signal. L^2 and $(L-2\,\text{mm})^2$ are also displayed for comparison, in *solid* and *dashed lines*, respectively

pret than pressure dependences, as the signal can vary at most as L^2 when perfect phase matching is obtained, and should increase at a lower rate or even oscillate (Maker fringes) in non-perfect phase-matching conditions. This is indeed the case between 1 and 2 mm of the medium; however, increasing further the cell length leads to a sharp signal increase, again steeper than a quadratic law. This shows that only part of the path within the cell leads to phase-matched generation. The dashed line shows a simple $(L-2\,\text{mm})^2$ law, which fits remarkably the data. This proves that phase matching is obtained in the cell between $z=2$ and $z=4$ mm. To the best of our knowledge, this is the first direct experimental demonstration of perfect phase matching in high-harmonic generation, based on a medium-length dependence. Previous claims of phase-matching demonstrations relied indeed either on modifications of the far-field profile or on pressure dependences mapped onto length dependences [9]. These results are completely consistent with those reported by Tamaki et al. [10]. However, the self-guiding effect invoked by Tamaki et al. was not obvious in those experiments. We therefore believe that it is the divergence of the laser beam by diffraction that explains the enhancement in phase matching. More investigations of the laser propagation in conditions optimizing high harmonics are under way.

4 Control of phase matching by manipulating the laser field by polarization optics

From the previous study it is obvious that being able to shape in intensity and phase the distribution of the laser field at focus opens ways to control phase matching, and optimize the generation process. While a thorough control would require many degrees of freedom, one may start with simple schemes adding one degree of freedom to modify the standard Gaussian beam.

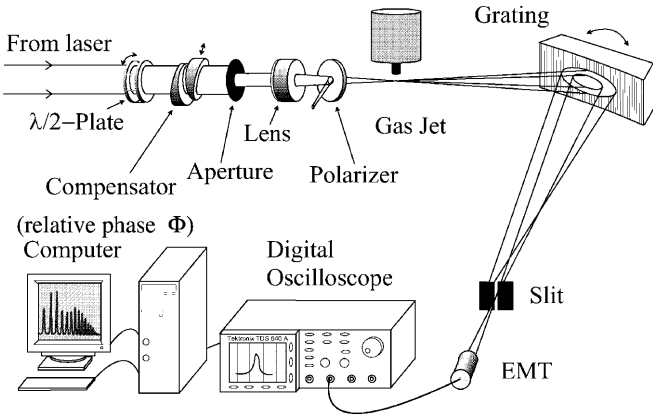

FIGURE 5 Experimental setup to manipulate the laser beam to control phase matching

One possibility is depicted in Fig. 5 [5]. A titanium–sapphire laser beam at the Lund Laser Facility is focused in a gas jet through a birefringent lens of 400-mm focal length. Two foci are therefore created, 7-mm apart, between which the energy can be distributed by means of an initial half-wave plate. We operated the experiment in a regime where this energy was balanced, meaning the incoming laser polarization was at 45 degrees from the lens axes. The lens birefringence induces spurious effects: first there is a time separation between the two orthogonal polarization components. This effect is compensated by introducing a Soleil–Babinet compensator, which also allows one to define and tune finely a relative phase between the two components. Finally the laser polarization after the lens should be elliptical; a polarizer brings it back to linear. A diaphragm inserted in the laser beam allows us to modify both the incoming energy and the confocal parameter of focusing.

In this setup, tuning the compensator phase changes completely the field distribution at focus, from one position roughly equivalent to having two laser beams with different foci interfering constructively on-axis at the middle of the foci, to another position where these two beams interfere destructively on-axis, in which case the energy is distributed far from the optical axis.

A phase matching map analysis shows that, in the experimental conditions just presented, a relative compensator phase of 4.8 rad results in a very large area of good phase matching on-axis, while a compensator phase of 3.4 rad degrades phase matching severely.

The experimental result is shown in Fig. 6. The optimum in phase matching corresponds very well to what is predicted by a phase matching map formalism. The solid line corresponds to an incoming energy of 4 mJ, and the dashed line of 5 mJ. The secondary maximum around 2 rad corresponds to a configuration where the on-axis intensity is high and the phase matching relatively poor. Figure 7 shows spectra obtained in neon when the gas jet is located 4 mm after the first focus, that is, almost centered between the foci. The solid line shows the two-foci case with 5 mJ on the target, and the dotted line the one-focus case with the gas jet located 4.5 mm after the focus, and an incoming energy of 3 mJ. These parameters are chosen to get identical peak intensities in the jet. Obviously, the conversion efficiency is better by a factor of at

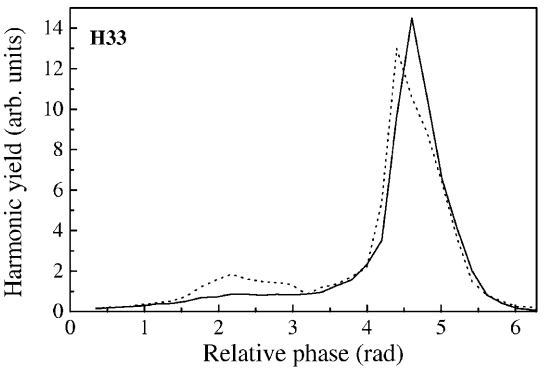

FIGURE 6 Harmonic yield versus the relative phase induced by the Soleil–Babinet compensator

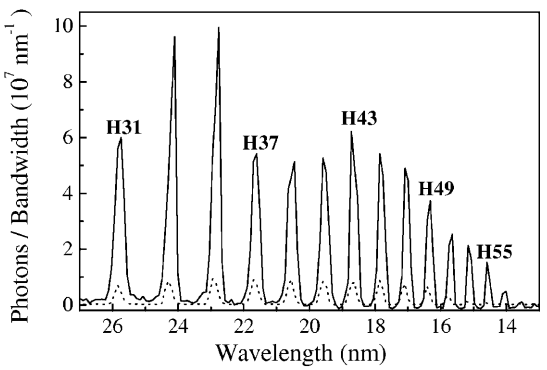

FIGURE 7 Comparison of spectra obtained in the two-foci case (*solid line*) and in the one-focus case (*dashed line*)

least four in the two-foci case. In other conditions, we could also observe an enhancement of one given harmonic (33rd harmonic) by a factor of two with respect to neighboring harmonics in the two-foci case, while it was about equal to them in the one-focus case.

This feasibility experiment demonstrates the interest of trying to shape the laser profile, to get full advantage of the possibilities opened by tailoring the atomic phase of high harmonics. The conversion efficiency measured with absolute XUV photodiodes ranged around 10^{-7} for the 33rd harmonic (50 eV).

5 Spatially coherent harmonics from solid targets

High harmonics from solids should in principle yield much higher conversion efficiencies. The principles are quite simple: in a non-relativistic regime, the incoming laser creates a plasma at the surface. The plasma electrons are then driven both by the laser, and by the plasma-restoring force, across the plasma-boundary region (Fig. 8a). If the latter is steep enough, then that motion can be strongly anharmonic, resulting in a series of even and odd harmonics. In contrast to high harmonics from gases, no plateau structure can be seen. If the laser intensity is increased further up to about 10^{18} W/cm^2, then the electron motion becomes relativistic. The Lorentz term becomes important, and starts to drive anharmonicities even in *s*-polarization. The occurrence of high harmonics in this regime can be simply modeled by a 'relativistic mirror' model (Fig. 8b). The collective electron motion is driven by the superintense laser forces $\boldsymbol{E} + \boldsymbol{v} \times \boldsymbol{B}$. The

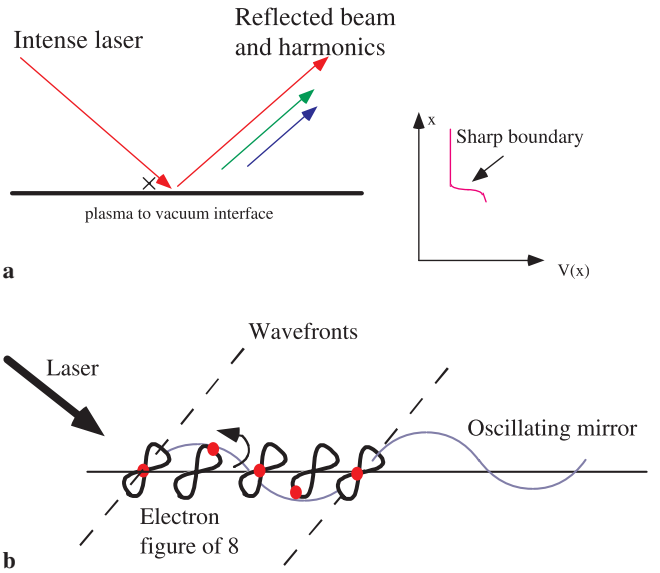

FIGURE 8 Principle of high-harmonic generation on solid surfaces: **a** in the non-relativistic plasma case; **b** in the relativistic case

laser light itself gets reflected onto this moving plasma surface, which induces large phase modulations and correspondingly very high harmonics [12]. The conversion efficiencies should be strongly enhanced in this regime.

In both cases, the plasma to vacuum interface should be very sudden, otherwise the anharmonic terms would vanish. As a result, the contrast ratio of the laser pulse should be excellent, to avoid the deleterious effects of a prepulse or pedestal causing an expanding preplasma, before the arrival of the main pulse.

Attempts to observe this new relativistic regime were performed with a 35-fs, multi-terawatt Ti–sapphire laser facility at Laboratoire d'Optique Appliquée, Palaiseau [8]. The irradiance on the target was 5×10^{17} W/cm^2, very close to the relativistic regime. The contrast ratio of the laser was 10^{-6} at 1 ps before the main pulse.

XUV light emitted in the specular direction was analyzed by a reflection-grating spectrometer, using as a detector a phosphor screen and a CCD. Figure 9 shows the long-wavelength side of a spectrum thus obtained using an op-

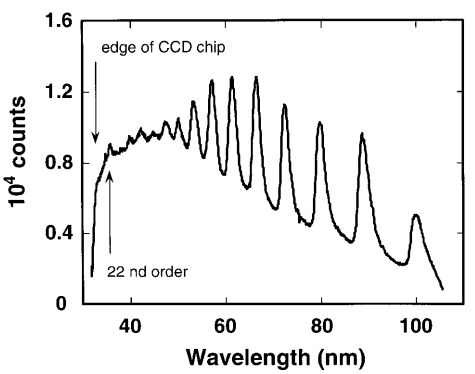

FIGURE 9 Long-wavelength side of the harmonic spectra obtained by shining a 35-fs pulse with an irradiance of 5×10^{17} W/cm^2 onto polished optical glass

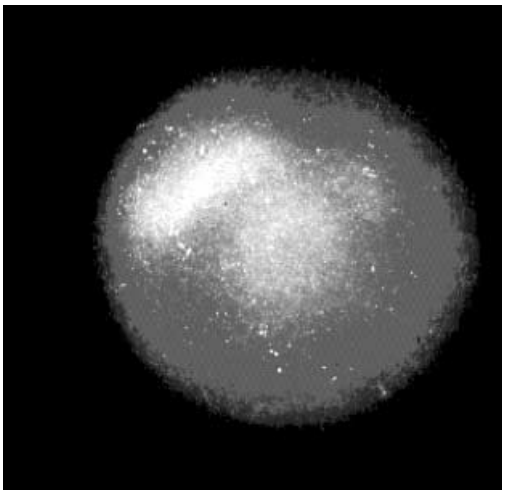

FIGURE 10 Spatial distribution of the harmonic radiation going through an aluminum filter, recorded on a phosphor screen, 10 cm from the target

tically polished glass target. Harmonics from the 8^{th} to the 22^{nd} orders are clearly visible. A signal was also observed at shorter wavelengths, down to the edge of our aluminum filters around 18 nm. This represents the shortest-wavelength harmonics on surfaces reported with femtosecond pulses. Those results were obtained in *p*-polarization; no signal was obtained in *s*-polarization.

Figure 10 shows an angular distribution of all harmonics going through the aluminum filter (from 18 to 80 nm). The short-wavelength beam is obviously well collimated, with a divergence between 50 and 100 mrad, slightly smaller than that of the laser. This result is in sharp contrast to that reported by Norreys et al. [7], and also to some measurements made at higher intensities, which were completely dominated by incoherent plasma light.

6 Conclusion

The results presented here show that new routes are explored to enhance photon yields at high harmonic frequencies. In gases, we have shown that novel phase-matching methods can strongly enhance the conversion efficiency in light noble gases like neon. Those methods do not rely on the positive atomic dispersion, but on the gradient of the atomic phase of the harmonics which, if carefully tailored, can compensate for the negative dispersion of a large density of free electrons.

In the long term, controlling precisely the spatial distribution of the laser at focus seems necessary. In a proof-of-principle experiment, we have shown that even a single additional degree of freedom improves significantly the process.

Harmonic generation by solids also seems very promising with femtosecond pulses; however the contrast ratio of present-day lasers does not seem sufficient to reach relativistic intensities at focus without creating a deleterious preplasma, so that no sign of relativistic behavior could be seen. Laser development is underway in several laser facilities to increase the contrast by several orders of magnitude, which should soon allow renewed efforts on this subject.

ACKNOWLEDGEMENTS This work was supported by the European Commission under contract ERBFM-GECT-950019.

REFERENCES

1 Y. Tamaki, O. Maya, K. Midorikawa, M. Obara: In Conf. Lasers Electro-Opt. 1998 (OSA Tech. Dig. Ser.) (OSA, Washington, DC 1998) Vol. 6, JTuA3
2 M. Schnürer, Z. Cheng, S. Sartania, M. Hentschel, G. Tempea, T. Brabec, F. Krausz: Appl. Phys. B **67**, 263 (1998)
3 A. Rundquist, C.G. Durfee, III, Z. Chang, C. Herne, S. Backus, M.M. Murnane, H.C. Kapteyn: Science **280**, 1412 (1998)
4 E. Constant, D. Garzella, P. Breger, E. Mével, C. Dorrer, C. Le Blanc, F. Salin, P. Agostini: Phys. Rev. Lett. **82**, 1668 (1999)
5 L. Roos, E. Constant, E. Mével, P. Balcou, D. Descamps, M.B. Gaarde, A. Valette, R. Haroutunian, A. L'Huillier: Phys. Rev. A **60**, 5010 (1999)
6 D. von der Linde, T. Engers, G. Jenke, P. Agostini, G. Grillon, E. Nibbering, A. Mysyrowicz, A. Antonetti: Phys. Rev. A **52**, R25 (1995)
7 P.A. Norreys, M. Zepf, S. Moustaizis, A.P. Fews, J. Zhang, P. Lee, M. Bakarezos, C.N. Danson, A. Dyson, P. Gibbon, P. Loukakos, D. Neely, F.N. Walsh, J.S. Wark, A.E. Dangor: Phys. Rev. Lett. **76**, 1832 (1996)
8 A. Tarasevitch, A. Orisch, D. von der Linde, P. Balcou, G. Rey, J.-P. Chambaret, U. Teubner, D. Klöpfel, W. Theobald: Phys. Rev. A **62**, 23 816 (2000)
9 M. Schnürer, Z. Cheng, M. Hentschel, G. Tempea, P. Kalman, T. Brabec, F. Krausz: Phys. Rev. Lett. **83**, 722 (1999)
10 Y. Tamaki, J. Itatani, Y. Nagata, M. Obara, K. Midorikawa: Phys. Rev. Lett. **82**, 1422 (1999)
11 P. Balcou, P. Salières, A. L'Huillier, M. Lewenstein: Phys. Rev. A **55**, 3204 (1997)
12 D. von der Linde, K. Rzazewski: Appl. Phys. B **63**, 449 (1996)